Progress In Electromagnetics Research C, Vol. 100, 83–93, 2020

Distributed Sensor Diagnosis in Twisted Pair Networks for Soft Fault Identification Using Reflectometry and Neural Network

Ousama Osman[1, *], Soumaya Sallem[1], Laurent Sommervogel[1], Marc Olivas Carrion[1], Pierre Bonnet[2], and Françoise Paladian[2]

Abstract—This paper aims at developing an approach allowing to detect, locate, and characterize soft faults (i.e., isolation damage) in branched network composed of shielded twisted pair (STP) cables. To do so, a distributed reflectometry diagnosis where several sensors (reflectometers) are placed at different ends of the network is used to maximize the diagnosis coverage. The soft fault identification is achieved by using Multi-Carrier Time Domain Reflectometry (MCTDR) combined with a Multi-Layer Perceptron Neural Network (MLP-NN). The main novelty here lies in the fact that the MLP-NN method is used for data fusion from several distributed reflectometers, which eliminates ambiguities related to the fault location. The required datasets for training and testing of the NN are generated by simulation. Simulation and experimental results are conducted to verify the effectiveness of the proposed approach for locating and characterizing the soft faults in branched networks.

1. INTRODUCTION

With the growing number of embedded electronic systems in today's means of transport and communication networks, the lengths of cables and the number of electrical interconnections are increasing. Whatever their application areas are, cables are always prone to faults and failures due to several internal and external conditions (mechanical vibration, thermal stress, moisture penetration etc.). These conditions cause the appearance of two types of faults, hard faults (open or short circuits), or soft faults (insulation damage, frays, cracks, etc.) [1]. The need for diagnosis methods and systems able to quickly detect and locate faults in early stage can greatly help in improving performances and avoiding dramatic accidents [2].

Several techniques have been suggested [3–5] in order to detect and locate faults before problem appearance. Reflectometry is considered as the best method for wire diagnosis [6]. However, despite its effectiveness in detecting and locating faults in a simple wired network, it remains limited in the case of branched networks. Indeed, using a single sensor cannot ensure the coverage of the entire network. This may be explained by the attenuation phenomenon [7] due to the traveled distance and multiple junctions encountered. In addition, the multitude of branches in the network causes a fault location ambiguity. Distributed diagnosis where several reflectometers are placed at different ends of the network under test (NUT) seems a good solution for these problems [8]. However, as several sensors are injecting their diagnostic signals simultaneously, specific signal processing methods are required to avoid interferences between them [9].

Recently, approaches based on time reversal (TR) principle [10, 11] have also been adopted to wiring fault detection and localization. The DORT (decomposition of the time reversal operator) method is certainly a more efficient one. The standard version of DORT (SDORT) as presented in [12] and the

Received 24 December 2019, Accepted 8 February 2020, Scheduled 21 February 2020
* Corresponding author: Ousama Osman (ousama.osman@win-ms.com).
[1] WinMs, 503, rue de Belvédère, ORSAY 91400, France. [2] Université Clermont Auvergne, CNRS, SIGMA Clermont, Institut Pascal, F-63000 CLERMONT-FERRAND, France.

enhanced version (EDORT) in [13] have shown promising results for locating single as well as multiple faults in different NUTs complexity. This is done by using several distributed vector network analyses (VNA). However, several factors might affect the practical implementation of the DORT technique in real-life applications such as noise, post-processing complexity, and the synchronization between different distributed VNAs which is a critical step. As a solution, the MCTDR [14, 15] has a huge advantage; it can precisely control the spectrum of the injected signals which allows a good performance (faults detection and localization) on distributed diagnosis. It enables real time monitoring of the wires without interfering with useful signals.

In this paper, we propose an adaptive multi-sensor data fusion method based on the MCTDR signal, which is combined with the MLP-NN for soft fault location and characterization in a complex wired network. In order to locate the defect and identify its type, each sensor performs a diagnosis and builds its own reflectogram by correlation between the incident signal and the reflected one. After that, the MLP-NN ensures the data fusion between different sensors. This proposed approach achieves more accurate and reliable results than approaches with a single sensor as in [16, 17].

Authors in [18] have proposed artificial neural networks (ANN) for the diagnosis of wired networks, where the whole Time Domain Reflectometry (TDR) response is processed, therefore the size of the required data is huge. In our work, the datasets are reduced since only the reflectogram most significant peaks are exploited, which reduces the number of neurons and prevents the over-fitting in NN.

This work is a follow-up to our recent awarded conference paper [19]. This article aims at validating the performance of the proposed approach by experimental results based on practical industrial elements. The results demonstrate that the new approach can merge the data from different sensors for locating and characterizing the soft faults in a complex wired network.

The rest of the paper is organized as follows. In Section 2 we explain the MCTDR reflectometry principle and the numerical model that describes the propagation of the wave along the lines of a network. Section 3 illustrates the procedures of the proposed method, the design and the training of the NN. Section 4 presents experimental results in order to evaluate the performance of the proposed method. Finally, the conclusions are drawn in Section 5.

2. PROPAGATION MODEL AND TEST SIGNAL

2.1. Theory of Transmission Line

A cable under test with high frequency signal can be treated as a transmission line, whose equivalent model with distributed RLGC (resistance, inductance, conductance, and capacitance per unit length) parameters [20] is illustrated in Figure 1, from which the well-known telegrapher's equations [21] are derived.

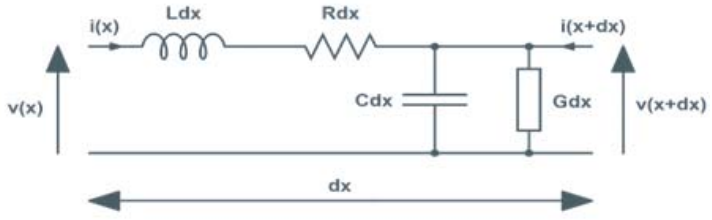

Figure 1. An RLGC model of a short cable portion of length dx.

In this work, the numerical simulations are performed thanks to an in-house code solving telegrapher's equations in the frequency domain. RLGC parameters take the following form in the simulation code [22]:

$$\begin{aligned} R &= R_0\sqrt{f} \text{ and } G = G_0 f \\ L &= L_0 + R_0/\left(2\pi\sqrt{f}\right) \text{ and } C = C_0 \end{aligned} \tag{1}$$

The parameters $R_0 = 8 \cdot 10^{-4}\,(\Omega/\mathrm{m})$, $L_0 = 596\,(\mathrm{nH/m})$, $C_0 = 97\,(\mathrm{pF/m})$, and $G_0 = 2.4 \cdot 10^{-11}\,(\mathrm{S/m})$ are different for every cable's type, and their values are affected by the geometry of the transmission line and by the electrical properties of the dielectrics and conductors. The signal propagation along the NUT is modeled as in [23], to provide its corresponding reflectometry response.

2.2. MCTDR Reflectometr

Similar to Radar, reflectometry injects a test signal into the NUT. This signal propagates along the network, and each impedance discontinuity met (connector, junction or fault [23]) reflects a part of its energy back to the injection point (Figure 2). The analysis of the reflected signal permits to detect, locate, and determine the type of these discontinuities.

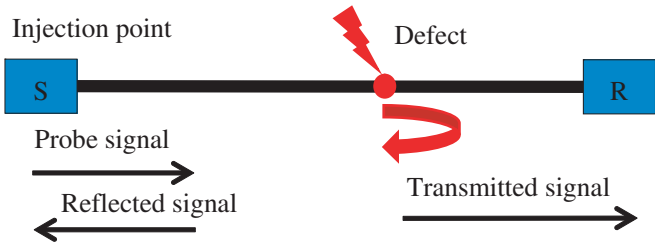

Figure 2. Reflectometry principle.

The position of an impedance discontinuity can be located by using the following equation:

$$d = \tau \cdot v_p/2 \tag{2}$$

where τ represents the measuring round trip time between the injection point and an impedance discontinuity, and V_p is the propagation speed in the cable.

Each discontinuity encountered by the test signal during its propagation is associated with a reflection coefficient. When the signal injected into a transmission line (with a characteristic impedance Z_c) encounters an impedance discontinuity Z_n during propagation, the corresponding reflection coefficient is given as follows:

$$\Gamma_n = (Z_n - Z_c)/(Z_n + Z_c) \tag{3}$$

For safety critical systems, more applications may require embedded diagnosis for real time monitoring and decision. Online diagnosis is then used while the target system is operating. Specific methods have been designed for this, such as MCTDR where a sum of a finite number of sinusoids at a given set of frequencies is injected into the cable under test.

$$s_k = \frac{2}{\sqrt{N}} \sum_{n=0}^{N/2} c_n \cos\left(\frac{2\pi n}{N} k + \theta_n\right) \tag{4}$$

Indeed, test signals must not interfere with the useful signals. To do so, the frequencies of subcarriers of the signal MCTDR are chosen outside the frequency bands used by the target system under test. Moreover, MCTDR has good autocorrelation properties (Figure 3) allowing a good accuracy of fault location.

3. PROPOSED APPROACH

The proposed work consists in automating the detection and location of soft faults in the branched network monitored by several reflectometers R_i $i \in \{1, 2, \ldots, N\}$, and N is the number of reflectometers. The considered wired network topology illustrated in Figure 4 was implemented using Twisted Pair cables with characteristic impedance $Z_c = 69\,\Omega$. The network is affected by two soft faults d_1 and d_2. The soft fault d_1 is located on the branch B_3 at 0.77 m from the junction J_1 and d_2 on the branch B_4 at 1.13 m from the junction J_2. We notice that the soft fault is represented

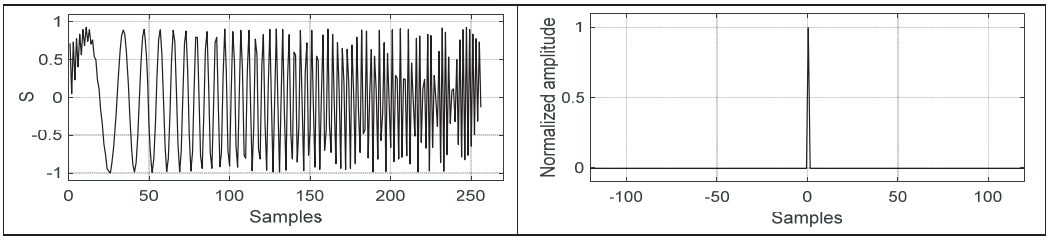

Figure 3. MCTDR signals: (a) Signal in the time domain and (b) autocorrelation function.

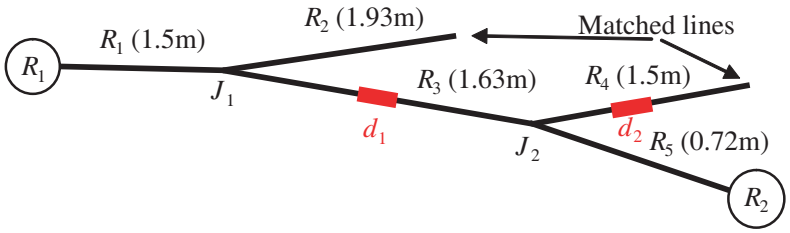

Figure 4. Complex wired network affected by two soft faults.

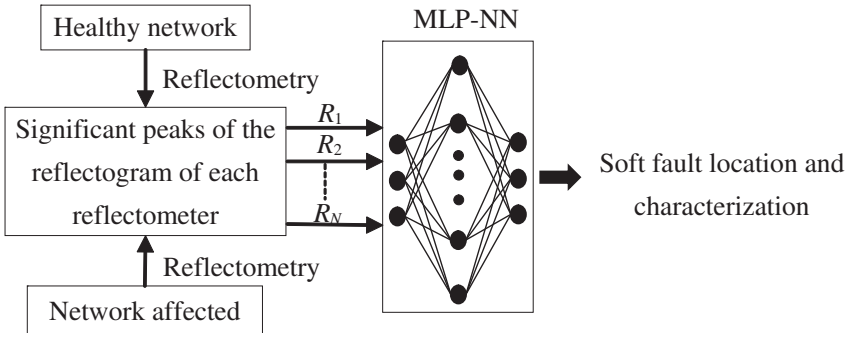

Figure 5. Block diagram of the fault location procedure.

by a localized change of characteristic impedance, with a length of $\Delta L = 3\,\text{cm}$ and an impedance $Z_d = Z_c(1 + \Delta Z_c)(20\% < \Delta Z_c < 30\%)$.

Figure 5 illustrates a block diagram of the fault location procedure. At first, to facilitate the reflectogram analysis, each sensor must calculate the difference between the response of a faulty network and that of a healthy one. This processing avoids the different peaks (variations) caused by the nodes in the network. Then, only the main peaks are detected, and for each peak, its magnitude and its position are stored. These peaks are then put into the MLP-NN; its output gives information about the location and the impedance of the soft faults.

In order to select the main peaks in the differential reflectogram, the detection thresholds represented by an exponential decay according to the cable's attenuation coefficient are used as follows:

$$\begin{aligned} Th_1 &= A_{\min} e^{-2\alpha X}/(1-\Gamma_0^2) \\ Th_2 &= -A_{\min} e^{-2\alpha X}/(1-\Gamma_0^2) \end{aligned} \tag{5}$$

where $X \in [0\,L]$; L is the maximum wire length from the sensor; $A_{\min} = 4 \cdot 10^{-3}$ is the sensor minimum detection threshold; $(1-\Gamma_0^2)$ is the coupling compensation term between the sensor and the network. The reflection coefficient Γ_0 is calculated as follows:

$$\Gamma_0 = (Z_c - Z_s)/(Z_c + Z_s) \tag{6}$$

where Z_s represents the source impedance, and Z_c is the characteristic impedance of the transmission line.

3.1. Design of Neural Network

The neural networks concept was inspired by biological neural networks. It is fast and flexible potentially able to model complicated functions and represent complex input/output relationships [24, 25]. Its training can be performed offline with a database including information about the state of the wired network. A fully connected three-layers (input, hidden and output) feed-forward neural network is used with a hyperbolic tangent activation function in the hidden layer and a linear activation function in the output one.

Figure 6 depicts the MLP-NN architecture, and the output layer of the network is composed of five neurons which correspond to the number of branches in the network. It is composed of two neural networks NN_1 and NN_2: NN_1 is used to locate the soft faults, and NN_2 is used to characterize their impedances. If a soft fault is detected, the corresponding NN_1 output gives the location (in m) of the soft fault on the faulty branch; otherwise, it is "zero". The corresponding NN_2 output gives the soft fault impedance (in Ω).

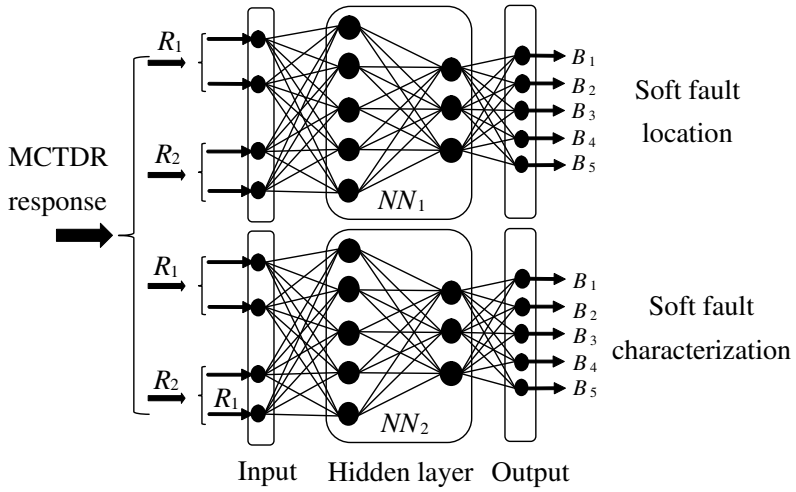

Figure 6. Soft fault location and characterization using MLP-NN.

The architecture type, number of neurons, and training dataset size play a key role in determining the best NN architecture [26]. The design of the NN has been achieved carefully with the appropriate number of hidden neurons. As a matter of fact, an NN having an insufficient number of neurons will not be able to learn the training database correctly. On the other hand, using too many neurons can lead to an overfitting phenomenon.

3.2. Training NN

The neural network was trained in MATLAB using NN-Toolbox with *Levenber-Marquard* [27] back-propagation training algorithm. The required datasets for training and testing the NN were created based on the MCTDR method. They are obtained from the simulation of soft faults randomly inserted in various scenarios (fault locations and fault resistances) in the wired network (Figure 7). The datasets are constituted from examples of reflectograms obtained by the reflectometers R_1 and R_2.

Nevertheless, in order to have a good learning process and test the effectiveness of the NN, the "split sample" method is used. It consists of dividing the datasets into three different subsets: training, validation, and test sets. Then, the NN is trained for different sizes (up to 100 hidden neurons in this study).

During the learning phase, an input-output set of data is fed into the network. For each of the inputs, the NN calculates the corresponding output and compares it with the correct one (target) which has been attributed to it. The connection weights between neurons are modified by an error measurement between produced and expected result. The error obtained at the output is reduced by the *Levenber-Marquardt* algorithm which is used to adapt the weights of the N. Finally, the generalization

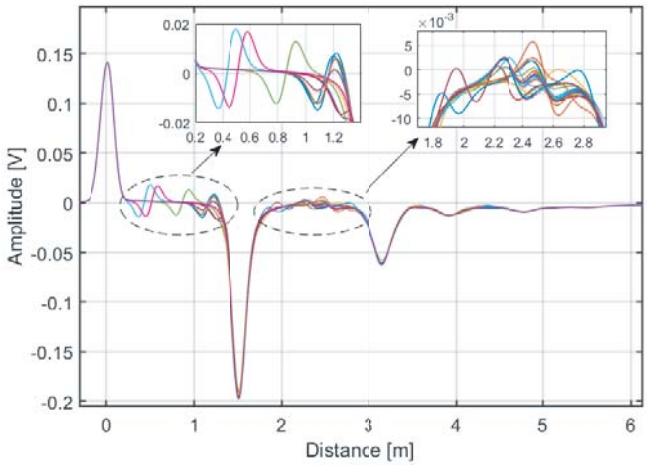

Figure 7. Simulated reflectograms obtained by the reflectometer R_1 show some examples of training data.

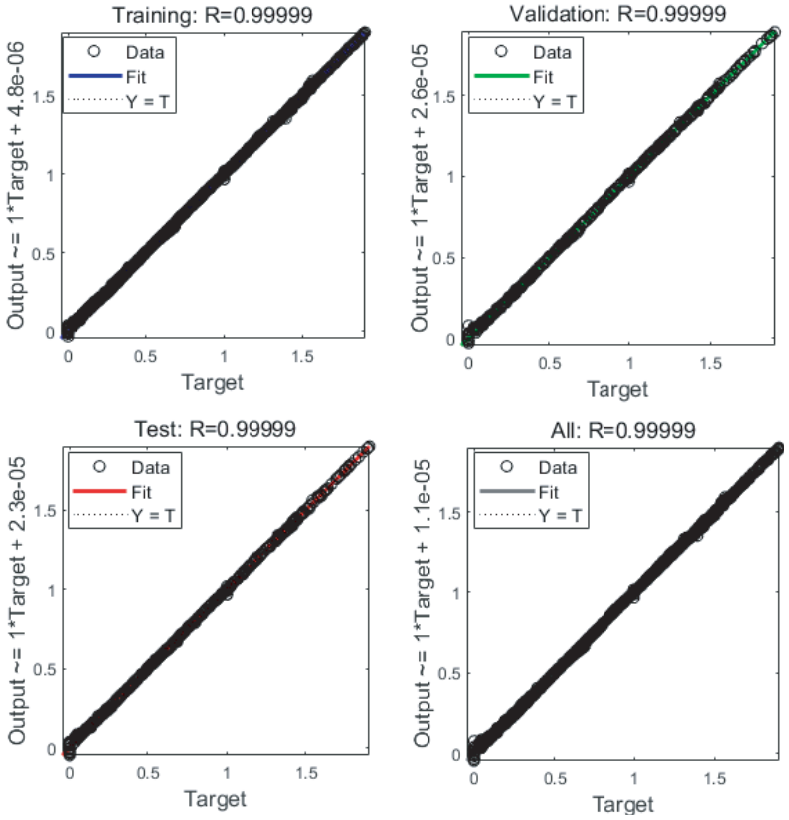

Figure 8. Regression fit of the output vs. targets during training, validation and test of the neural network.

capability of the NN is assessed by calculating the Mean Square Error (MSE) obtained in the test set which evaluates the quality of the estimation of the NN. The NN training time, with a data set about 40000 examples, is about 2h10 using a PC equipped with Intel core i5-4460 and 8 Gb of RAM.

After training the NN, its performance is checked by plotting the linear regression that relates the targets (soft fault positions) to the outputs as shown in Figure 8 which shows a satisfactory correlation between them.

It should be noted that the creation of the needed database may require a relatively long time, depending on the NUT topology and the number of parameters used (hidden layer, neurons, etc.). However, it can be performed "offline", the diagnosis of the wired network using the trained NN is very fast and can be achieved "online".

4. EXPERIMENTAL VALIDATION

To illustrate the performance of the proposed method, the following section presents an experimental setup. We opted to experimentally test the network presented in Figure 4 which is composed of 5 branches connected via two junctions.

4.1. Measurement Setup

The considered NUT of Figure 4 was implemented using an aeronautical cable MLB24 (shield twisted pair (STP) cable of type EN 2714-013). The extremities of the network are matched to the characteristic impedance of the lines. The MCTDR responses of the NUT is measured by two specific reflectometers R_1 and R_2 (output signal $< 1\,\text{V}$, output impedance $50\,\Omega$ and bandwidth ranging from 300 kHz to 200 MHz). The MCTDR reflectometry is integrated in a Field-Programmable Gate Array (FPGA) developed by WIN-MS (Wire Network Monitoring Solutions) company. Each sensor features wireless communication capability to send information to a tablet PC. A graphical user interface (GUI) (running under Android/Windows platform) controls the injection/acquisition procedure of the diagnosis signal and displays the received reflectograms. In the case of distributed diagnosis, each sensor performs a diagnosis and constructs its own reflectogram. The data are then sent to the tablet PC which is used for running the trained neural network. The whole experimental setup is illustrated in Figure 9.

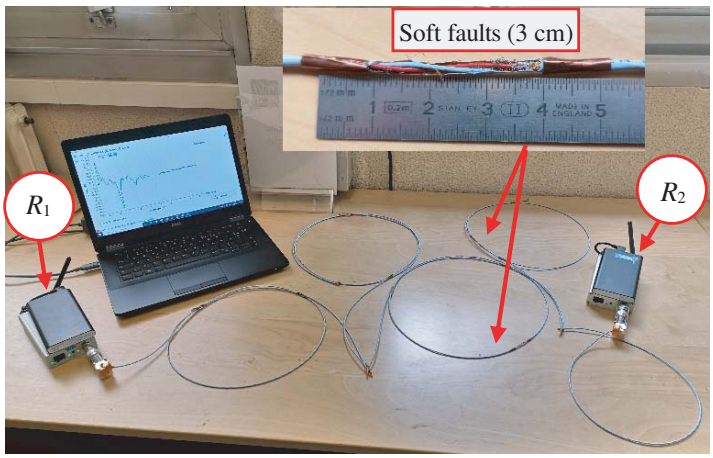

Figure 9. Implementation of the NUT in Figure 4 using STP EN 2714-013 MLB24 cables and connected to the reflectometers R_1 and R_2 for performing the MCTDR measurement.

4.2. Results and Discussions

To validate the propagation model, we rely on the wired network of Figure 4. Figure 10 shows the reflectometry response of the healthy network by the reflectometers R_1 and R_2, respectively. They

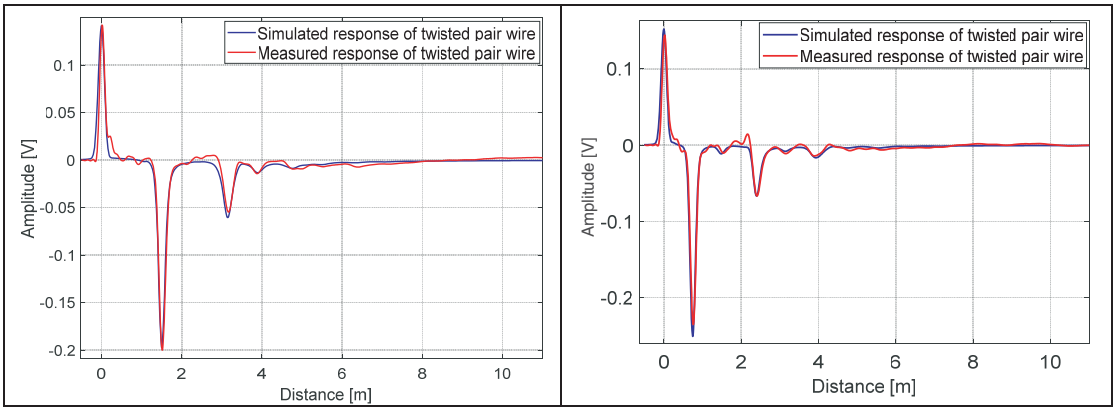

Figure 10. Comparison between simulation results and measures for the MCTDR response of healthy network obtained by the reflectometers (a) R_1 and (b) R_2.

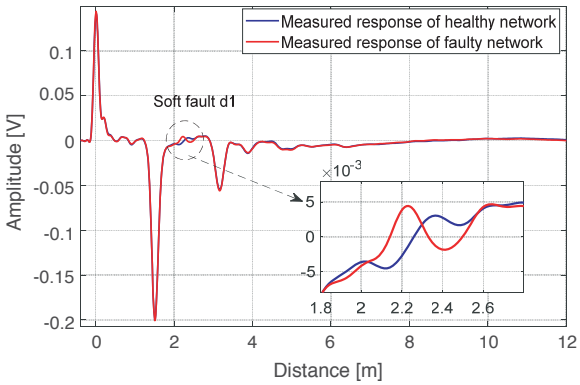

Figure 11. The measured MCTDR response of a healthy and a faulty network obtained by the reflectometer R_1.

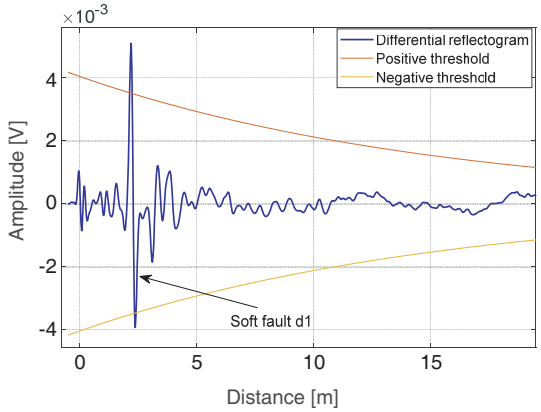

Figure 12. Difference between the response of a faulty and a healthy network obtained by the reflectometer R_1.

illustrate a good agreement between measurement and simulation results, both for positions and amplitudes of the main peaks. The difference between the simulated and measured values may be due to the imperfect numerical modeling of the network ($RLCG$ geometrical and electrical uncertainties), and also to the impedance of the connection (nodes, the coupling between the sensor and the network).

By observing Figure 11 and Figure 12, the reflectometer R_1 locates the soft fault d_1 at a distance of 2.2 m, and it can be located on either branch B_2 or B_3. In this case, we have a fault location ambiguity. The soft fault d_2 is not detected by R_1 because of the attenuation phenomenon. The reflectometer R_2 on its side locates the soft fault d_1 at 1.53 m and d_2 at 1.85 m (Figure 13 and Figure 14), and they can also be located on either branch B_3 or B_4.

Accordingly, to remove any soft fault location ambiguity on the network, the data fusion between R_1 and R_2 using MLP-NN is necessary. The measured data are post-processed using the proposed approach in Section 3. Table 1 shows the estimated data obtained at the output of the both NNs. Each one contains 48 neurons in the hidden layer and is trained by 40000 examples. We can clearly see in Table 1 that the estimated soft fault positions and impedances by the trained NNs are close to the injected ones with relative error less than 3%.

The results presented in Table 1 confirm the efficiency of our proposed approach to merge data between the reflectometers in order to locate and characterize the soft faults in the branched network. It is shown that MLP-NN yields some errors in the location and the characterization of the soft faults. The

accuracy can be enhanced by increasing the reflectogram point's number and the number of examples in the database as well as optimizing the number of neurons in the hidden layer.

Briefly, the proposed approach has many advantages over the existing approaches such as:

- The proposed method combining the MCTDR reflectometry with the MLP-NN enables data fusion from several distributed reflectometers for better locating faults in branched networks without ambiguities.
- Working with the most significant peaks of differential reflectogram rather than the whole reflectometry response (as in [13]), which reduces the size of the required data, consequently reduces the number of neurons in hidden layer, the time of processing, and prevents the over-fitting in NN.
- The distribution of the sensors at different extremities provides a complete coverage of the network and cancels the fault location ambiguity.
- Optimizing computational time diagnosis. The diagnosis can be achieved online, and the time to obtain the state of the wired network using trained NN remains less than 1 s.

Table 1. Estimated results at the output of the neural networks.

	Position and impedance of the actual soft fault	Estimated soft fault positions by NN_1 (m)	Estimated soft fault impedances by NN_2 (Ω)	Relative position error (%)
B_1	No soft fault	0.03	69	-
B_2	No soft fault	0.03	70	-
B_3	0.77 m from J_1 with $Z_d = 90\,\Omega$	0.78	89	1.29
B_4	1.13 m from J_2 with $Z_d = 90\,\Omega$	1.1	86	2.65
B_5	No soft fault	0.03	69	-

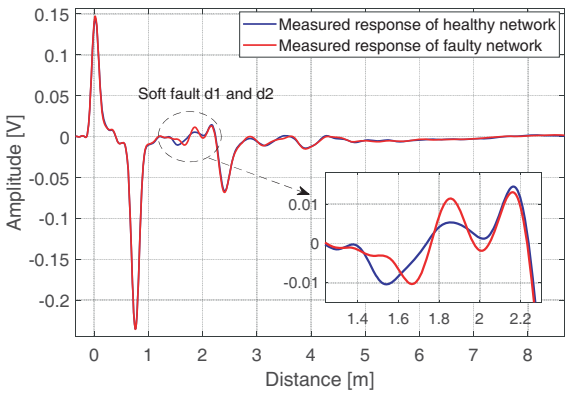

Figure 13. The measured MCTDR response of a healthy and a faulty network obtained by the reflectometer R_2.

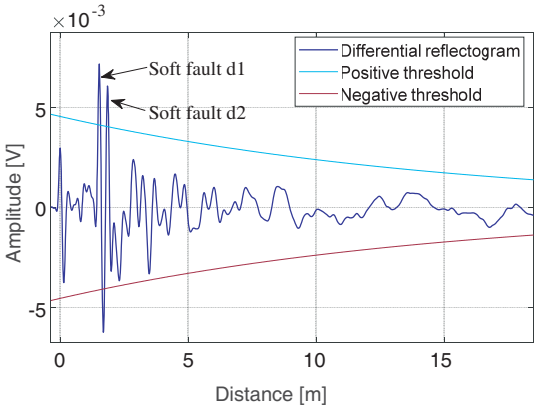

Figure 14. Difference between the response of a faulty and a healthy network obtained by the reflectometer R_2.

5. CONCLUSION

In this paper, we have presented a new approach for the diagnosis of wired networks. This approach combines the MCTDR test signal with the MLP-NN in order to solve ambiguity problems for soft fault location and characterization in branched networks. The NN ensures data fusion from several sensors placed at different ends of the network. The NN is trained using only significant peaks of the reflectogram of each sensor. This leads to a reduction of the size of the dataset and consequently reduces the number of neurons and the processing time.

In the case of an embedded diagnostic system, the training of NN can be performed offline, while the healthy state of the wired network can be obtained in real-time. Simulated and experimental results have proved the efficiency of the proposed technique in precisely detecting, locating, and characterizing multiple soft faults in the branched networks.

Future work will focus on integrating the communication between sensors using the phase modulation of the diagnosis signal. This communication improves the diagnosis quality and ensures data fusion from several reflectometers for an optimized distributed diagnosis without any ambiguities.

REFERENCES

1. Griffiths, L. A., R. Parakh, C. Furse, and B. Baker, "The invisible fray: A critical analysis of the use of reflectometry for fray location," *IEEE Sensors Journal*, Vol. 6, No. 3, 697–706, 2006.
2. Schuet, S., D. Timucin, and K. Wheeler, "A model-based probabilistic inversion framework for characterizing wire fault detection using TDR," *IEEE Trans. Instrum. Meas.*, Vol. 60, No. 5, 1654–1663, May 2011.
3. Shin, Y. J., et al., "Application of time-frequency domain reflectometry for detection and localization of a fault on a coaxial cable," *IEEE Trans. Instrum. Meas.*, Vol. 54, No. 6, 2493–2500, Dec. 2005.
4. Shi, Q. and O. Kanoun, "Wire fault diagnosis in the frequency domain by impedance spectroscopy," *IEEE Trans. Instrum. Meas.*, Vol. 64, No. 8, 2179–2187, Aug. 2015.
5. Lelong, A., M. Olivas Carrion, V. Degardin, and M. Lienard, "On line wiring diagnosis by modified spread spectrum time domain reflectometry," *PIERS Proceeding*, 182–186, Hangzhou, China, Mar. 24–28, 2008.
6. Auzanneau, F., "Wire troubleshooting and diagnosis: Review and perspectives," *Progress In Electromagnetics Research B*, Vol. 49, 253–279, 2013.
7. Osman, O., S. Sallem, L. Sommervogel, M. Olivas Carrion, A. Peltier, P. Bonnet, and F. Paladian, "Method to improve fault location accuracy against cables dispersion effect," *Progress In Electromagnetics Research Letters*, Vol. 83, 29–35, 2019.
8. Ben Hassen, W., F. Auzanneau, L. Incarbone, F. Pérès, and A. François, "Distributed sensor fusion for wire fault location using sensor clustering strategy," *International Journal of Distributed Sensors Networks*, 1–17, 2015, ISSN 1550-1329.
9. Lelong, A., L. Sommervogel, N. Ravot, and M. Olivas Carrion, "Distributed reflectometry method for wire fault location using selective average," *IEEE Sensors Journal*, Vol. 10, No. 2, 300–310, Feb. 2010.
10. El Sahmarany, L., L. Berry, N. Ravot, F. Auzanneau, and P. Bonnet, "Time reversal for soft faults diagnosis in wire networks," *Progress In Electromagnetics Research M*, Vol. 31, 45–58, 2013.
11. Kafal, M., R. Razzaghi, A. Cozza, F. Auzanneau, and W. Ben-Hassen, "A review on the application of the time reversal theory to wire network and power system diagnosis," *IEEE International Instrumentation and Measurement Technology Conference*, Auckland, New Zealand, May 2019.
12. Abboud, L., A. Cozza, and L. Pichon, "A non-iterative method for locating soft faults in complex wire networks," *IEEE Transactions on Vehicular Technology*, Vol. 62, No. 3, 1010–1019, 2013.
13. Kafal, M., A. Cozza, and L. Pichon, "Locating multiple soft faults in wire networks using alternative DORT implementation," *IEEE Transactions on Instrumentation and Measurements*, Vol. 65, No. 2, 399–406, 2015.

14. Lelong, A. and M. Carrion, "On line wire diagnosis using multi-carrier time domain reflectometry for fault location," *2009 IEEE Sensors*, 751–754, Oct. 2009.
15. Sallem, S. and O. Osman, "Wired network distributed diagnosis and sensors communications by Multi-carrier Time Domain reflectometry," *IEEE Intelligent Systems Conference*, London, UK, Sep. 2018.
16. Amloune, A., H. Bouchekara, M. K. Smail, F. de Paulis, et al., "An intelligent wire fault diagnosis approach using time domain reflectometry and pattern recognition network," *Nondestructive Testing and Evaluation*, 2018, DOI: 10.1080/10589759.2018.1559312.
17. Laib, A., M. Melit, B. Nekoul, K. E. K. Drissi, and K. Kerroum, "Soft fault identification in electrical network using time domain reflectometry and neural network," *LNEE Lecture Notes in Electrical Engineering*, 365–376, Springer, Jan. 2019.
18. Smail, M. K., T. Hacib, L. Pichon, and F. Loete, "Detection and location of defects in wiring networks using time domain reflectometry and neural network," *IEEE Trans. on Magn.*, Vol. 47, No. 5, 1502–1505, May 2011.
19. Osman, O., S. Sallem, L. Sommervogel, M. Olivas, et al., "Distributed sensor diagnosis in complex wired networks for soft fault detection using reflectometry and neural network," *IEEE Autotestcon*, USA, Aug. 2019.
20. Tang, H. and Q. Zhang, "An inverse scattering approach to soft fault diagnosis in lossy electric transmission lines," *IEEE Transactions on Antennas and Propagation*, Vol. 59, No. 10, 3730–3737, Nov. 2011.
21. Hayt, W., *Engineering Electromagnetics*, 6th edition, 437–440, McGraw-Hill, 1989.
22. Zhang, J., Q. B. Chen, Z. Qiu, J. L. Drewniak, and A. Orlandi, "Extraction of causal RLGC models from measurements for signal link path analysis," *2008 International Symposium on Electromagnetic Compatibility — EMC Europe*, 1–6, Hamburg, 2008.
23. Ravot, N. and F. Auzanneau, "Defects detection and localization in complex topology wired networks," *Ann. Telecommun.*, Vol. 62, Nos. 1–2, 193–213, Jan. 2007.
24. Coccorse, E., R. Martone, and F. C. Morabito, "A neural network approach for the solution of electric and magnetic inverse problems," *IEEE Trans. Magn.*, Vol. 30, No. 5, 2829–2839, Sep. 1994.
25. Travassos, L., D. A. G. Vieira, N. Ida, C. Vollaire, and A. Nicolas, "Characterization of inclusions in a nonhomogenous GPR problem by artificial neural networks," *IEEE Trans. Magn.*, Vol. 44, No. 6, 163–1633, Jun. 2008.
26. Zhou, Y., J. Hahn, and M. S. Mannan, "Fault detection and classification in chemical processes based on neural networks with feature extraction," *ISA Transactions*, Vol. 42, 651–664, 2003.
27. Lingling, M., F. Xu, et al., "Earthquake prediction based on levenberg-marquardt algorithm constrained back-propagation neural network using DEMETER data," *Proceedings of the 4th International Conference on Knowledge Science, Engineering and Management*, 591–596, Belfast, Northern Ireland, UK, Sep. 2010.